Impedance Spectroscopy analysis of Ti_nO_{2n-1} Magnéli phases

D. Regonini[1*], A.C.E. Dent[1], C. R. Bowen[1], S. R. Pennock[2] and J. Taylor[2]

[1]*Materials Research Centre, Department of Mechanical Engineering, University of Bath (UK)*

[2]*Department of Electronic & Electrical Engineering, University of Bath (UK)*

**Corresponding Author:*

Domenico Regonini

Materials Research Centre, Dept. Mechanical Engineering

Claverton Down Road, BA2 7AY, Bath, (UK)

Tel. +44 (0)1225 383062

d.regonini@bath.ac.uk,

Abstract

This letter presents a comprehensive impedance spectroscopy characterisation of Magnéli phases (Ti_nO_{2n-1}) over a range of temperatures, which are of interest in electrochemistry and sensing applications, with the aim to enhance the understanding of their electrical properties and influence their microstructure. The impedance of the Ti_nO_{2n-1} can be resolved into two different contributions, namely the grain bulk (R_B) and grain boundaries (R_{GB}). The ac conductivity increases with frequency and temperature, following a universal power-law. The high relative permittivity (10^5-10^6), which is relatively frequency independent from 0.1Hz to 100kHz, is attributed to the presence of insulating grain boundaries (R_{GB}>>R_B) creating an Internal Barrier Layer Capacitor (IBLC) effect. Above 100kHz, the grain boundaries begin to contribute to the ac conductivity and the permittivity drops sharply.

Keywords: electrical properties, grain boundaries, electroceramics

1. Introduction

It is well known that the electrical conductivity of titanium dioxide can be enhanced by heat-treating the oxide at high temperature in a reducing atmosphere, usually in the presence of hydrogen or carbon. This process leads to the formation of sub-stoichiometric oxides with the general formula Ti_nO_{2n-1} (with $3 < n < 10$), known as Magnéli phases [1]. In non-stoichiometric titanium dioxide, TiO_{2-x}, with low x ($0 < x < 0.10$), the dominant point defects in the structure consist of Ti^{3+} and Ti^{4+} interstitials and oxygen vacancies [2]. However the Magnéli phases (x=0.10-0.34) are characterised by extended planar defects and crystallographic shear planes which vary according to the oxygen deficiency [3-4]. Magnéli phases are of interest in cathodic protection, batteries, catalytic support for fuel cells, treatment of aqueous waste and contaminated water due to their high electrical conductivity and chemical resistance [5-7].

A comprehensive understanding of the electrical properties of Magnéli phases is crucial to the progress of the above-mentioned fields. The dc electrical conductivity of Ti_nO_{2n-1} with $3 \leq n \leq 6$ has been studied by Bartholomew and Frankl from 78-298K [8]. Inglis *et al.* [9] performed a similar study for $4 \leq n \leq 9$ at 4-320K. In both studies, a transition in the conductive mechanism from semiconducting to metallic was observed at ~150K. The ac electrical properties of Ti_nO_{2n-1} have not been extensively investigated and in this letter we discuss the manufacture and microstructure of Magnéli phases along with impedance spectroscopy (IS) of the frequency and temperature dependence of ac conductivity and relative permittivity (ε_r).

2. Experimental Methods

The TiO_2 powder (3µm, Pikem, 99.5%) was processed by adding 3wt.% of Polyethylene Glycole (PEG) 8000MW to distilled water to create a slurry which was ball-milled for 24h. The slurry was dried and the resulting powder sieved through a 45µm mesh. Pellets were formed by uniaxial pressing at 200MPa. The green bodies were then fired at 1300°C (4h) and reduction of TiO_2 was achieved by carbothermal reduction at 1300°C (6h). Typical sample dimensions were 10.6mm diameter (ϕ), and 1.4mm thickness (t). For electrical measurements samples were polished to a mirror finish and electroded with Au using an Edward E306 Evaporator. The ac conductivity and permittivity were measured from 25-375ºC using a Solartron 1260 Impedance Analyser with a Solartron 1296 dielectric interface. The range of frequency investigated was from 0.1Hz to 1MHz, and the applied voltage was $0.1V_{rms}$. Microstructural characterisation was undertaken by using optical microscopy and a Scanning Electron Microscope (SEM) and X-ray diffraction (XRD). The density of the tablets was obtained using the hydrostatic method (BS Standard No. EN 623-2:1993).

3. Discussion and Results

The microstructure of a typical Ti_nO_{2n-1} specimen thermally etched in argon, **Fig. 1a,** reveals a dense structure, calculated to be 95 to 95.5% of theoretical density (4.3 g/cm^3) [6]. The presence of large grains, over 30µm, is clearly observed in **Fig.1a**, suggesting that a degree of grain growth has occurred during the reduction treatment of TiO_2. For comparison, the grain size of non-reduced TiO_2 was typically in the order of 10µm (not shown). The residual porosity (5%) measured is similar to the low porosity observed in the SEM image, **Fig. 1b**.

A representative XRD spectrum of the Ti_nO_{2n-1} specimens, **Fig.2a,** reveals the presence of several Magnéli phases, which can be indentified by their characteristic peaks and the main phases present are Ti_4O_7 (20.7° and 31.7°), Ti_5O_9 (21.95°), Ti_6O_{11} (22.85°), which are the most electrically conductive of the series [6, 10]. The XRD spectrum of TiO_2 is also shown for comparison in **Fig. 2b,** revealing the presence of residual TiO_2 within the reduced Ti_nO_{2n-1} samples. As a result, the electrical conductivity of our specimens is expected to be few orders of magnitude lower than for pure Ti_4O_7, Ti_5O_9 and Ti_6O_{11}, reported to be in the order of 10^3-10^5 S/m [5-7].

The impedance plot for $Ti_nO_{2n-1,}$ **Fig. 3**, can be interpreted as the result of two RC elements in series, where the non-zero intercept at high frequency (inset of **Fig. 3**) provides an estimation of the resistance of the bulk of the grains (R_B) [11], which is approximately 12Ω and taking into account the size of the specimens corresponds to a resistivity of 10^{-1} Ω·m. The intercept, $R_{B,}$ is not significantly affected by the temperature and, as expected considering the residual TiO_2, the resistivity is 2 to 4 orders of magnitude higher than values reported for pure Magnéli Phases [5-7]. The semicircle for the grain bulk is not observed at room temperature (RT) or higher temperature because the relaxation time ($\tau = RC$) of the grain bulk regions is at a frequency higher than 1MHz. The only observable arc in **Fig 3** appearing in the region 100kHz-0.1Hz is assigned to the grain boundary response (R_{GB}) [12] and corresponds to a resistance of approximately 1400 Ω and a resistivity of 10^2 Ω·m at room temperature. At room temperature R_{GB} is therefore approximately three orders of magnitude higher than $R_{B;}$ however since R_{GB} decreases systematically with increasing temperature it eventually approaches R_B (~10^{-1} Ω·m) at 375°C.

It is interesting to observe how the real ac conductivity, $\sigma(\omega)$, of Ti_nO_{2n-1} varies with frequency, as shown in **Fig. 4**. There is no frequency dependence of the conductivity at

low (0.1Hz) and medium (1kHz) frequencies, whereas for higher (1-10kHz) frequencies the conductivity begins to rise with frequency and the same trend is observable over the all range of temperatures investigated. The lower the magnitude of the conductivity (i.e. at lower temperature), the earlier it becomes frequency dependent, following the "universal" power law behaviour [13] of the type $\sigma(\omega) = \sigma(0) + B\omega^p$, where ω is the angular frequency ($2\pi f$), p a constant between 0 and 1, and $\sigma(0)$ the conductivity at low frequency (also identified as σ_{dc}, dc conductivity). It has been previously shown that power law dispersions in conductivity and permittivity can be explained at a microscopic level by a resistor-capacitor (RC) network without the need to introduce novel many-body relaxation phenomena [14].

In the particular case of Magnéli phases the resistors in the RC network are represented by sites in which the oxygen has been stripped out during the carbothermal treatment to generate $Ti_nO_{2n-1,}$ whereas the stoichiometric and more resistive TiO_2 areas correspond to the capacitative sites. This is supported by the XRD analysis, that indicated the ceramic is such a mixture. Based on this assumption we would also expect a similar, but opposite, power law dispersion of the relative permittivity (ε_r) of the Magnéli phases, with a decrease of the permittivity with frequency with ε_r approaching a constant value at higher frequency (>10kHz). However, it is observed in **Fig. 5**, especially at low temperatures (<300°C), that there is only a slight decrease of the relative permittivity with frequency in the range 1Hz to 100kHz, followed by an abrupt decrease at frequencies higher than 100kHz. Interestingly, the impedance plot in **Fig. 3**, suggests that the grain boundary response for Ti_nO_{2n-1} occurs in the region 0.1Hz to 100kHz. The abnormally high relative permittivity (10^5-10^6) and its lack of frequency dependence over the 1Hz to 100kHz range, particularly at low temperature (<300°C), can be explained by the presence of insulating grain boundaries, with a R_{GB} resistivity two to

three orders of magnitude higher than R_B, creating an Internal Barrier Layer Capacitor (IBLC) effect [15]. A possible reason for the presence of more resistive grain boundaries is that the reduction of TiO_2 occurs preferably in the bulk of the grains rather than at the interface between grains, although further analysis are required to confirm this hypothesis. The significant drop of the permittivity at higher frequencies (100kHz-1MHz) is thought to occur when the more resistive intergranular regions also begin to contribute to the network conductivity. The drop of the permittivity is more dramatic at lower temperature (<300°C) because at higher temperatures (>300°C) the resistivity of the grain boundaries decreases and R_{GB} approaches R_B. As a consequence the IBLC becomes less significant and a power law behaviour of the type $\varepsilon(\omega) = D\omega^{p-1} + \varepsilon_\infty$, where D is a constant and ε_∞ is the limit of permittivity at high frequency, is instead observed.

4. Conclusions

The microstructure, X-ray analysis and Impedance Spectroscopy (IS) characterisation of Ti_nO_{2n-1}, has been presented, with the objective to enhance the understanding of ac electrical properties of these materials. The reduced specimens contain a mixture of Ti_nO_{2n-1} phases and some unreduced TiO_2 with a dc conductivity 7-8 orders of magnitude higher than pure TiO_2 at room temperature. The ac conductivity increases with frequency (and temperature) following a power law dispersion, as expected for a material which can be modelled by a RC network. However the relative permittivity, especially at low temperatures (<300°C), is less frequency dependent due to the presence of grain boundaries three orders of magnitudes more resistive than the grain

bulk. This suggests that intra-grain reduction is favoured over inter-grain reduction and as a result an Internal Barrier Layer Capacitor (IBLC) effect is produced. Further work in evaluating activation energies for conduction for stoichiometric and non-stoichiometric titania based materials is currently in progress [16].

Acknowledgements

The research leading to these results was funded from the European Union Seventh Framework Programme (FP7/20072013) under grant agreement n° CP-TP 229099-2 as part of the 'MesMesh' project.

References

1. S. Andersson, A. Magnéli, Naturwiss **43**, 495-496 (1956).
2. E. G. Seebauer, and M. C. Kratzer, Mater. Sci. Eng. Rep. R: **55**, 57-149, (2006).
3. S. Harada, K. Tanaka, and H. Inui, J. Appl. Phys. **108**, 083703-1-6 (2010).
4. L. Liborio, and N. Harrison, Phys. Rev. B **77**, 104104-1-10 (2008).
5. P. C. Hayfield, Development of a New Material - Monolithic Ti_4O_7 Ebonex Ceramic. Cambridge: Royal Society of Chemistry (2002)
6. F. C. Walsh, and R. G. A. Wills, Electrochim. Acta **55**, 6342-6351 (2010).
7. J. R. Smith, F. C. Walsh, and R. L. Clarke, J. Appl. Electrochem. **28**, 1021-1033 (1998).
8. R. F. Bartholomew, and D. R. Frankl, Phys. Rev. **187**, 828-833 (1969).

9. A. D. Inglis, Y. L. Page, P. Strobel, and C. M. Hurd, J. Phys. C; Sold. State Phys. **16**, 317-333 (1983).
10. L. M. Vračar, N. V. Krsajić, V. R. Radmilović, and M. M. Jakšić, J. Electroanalytical Chem. **587**, 99-107 (2006).
11. D. C. Sinclair, T. B. Adams, F. D. Morrison, and A. R. West, Appl. Phys. Lett. **80**, 2153-2155 (2002).
12. J. E. Bauerle, J. Phys. Chem. Solids **30**, 2657-2670 (1969).
13. A. K. Jonscher, Nature **267**, 673-679 (1977).
14. D. P Almond, and C. R. Bowen, Phys. Rev. Lett. **92**, 157601-1-4, (2004).
15. M. Li., Z. Shen, M. Nygren, A. Feteira, D. C. Sinclair, and A. R. West, J. Appl. Phys. **106**, 104106-1-8 (2009).
16. D. Regonini, A.C.E. Dent, C. R. Bowen, S. R. Pennock and J. Taylor, to be published.

Figure Captions

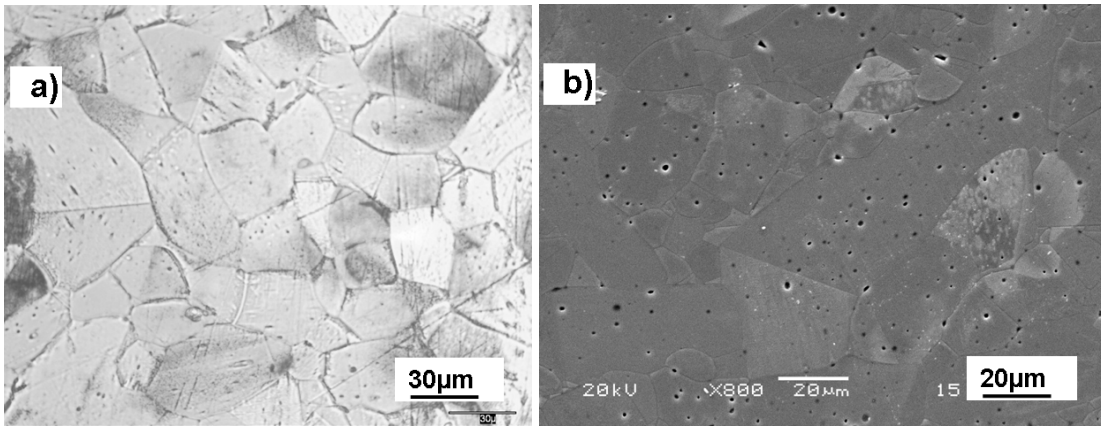

Figure 1. Optical **(a)** and SEM **(b)** images of the microstructure of thermally etched Magnéli Phases.

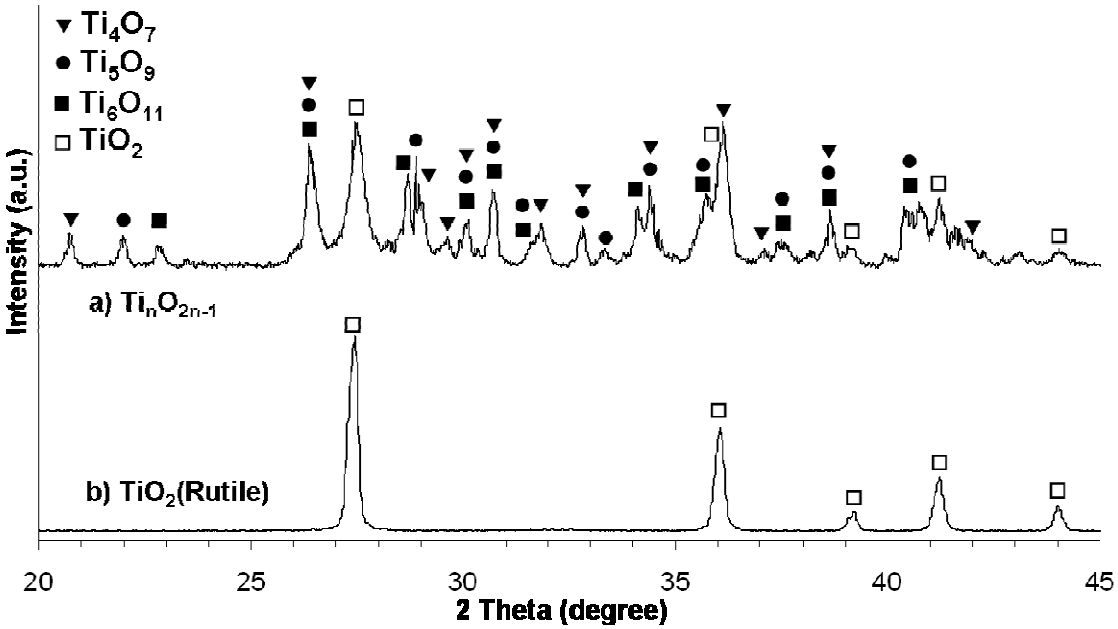

Figure 2. XRD spectra of Ti_nO_{2n-1} obtained from carbothermal reduction **(a)** and TiO_2 before the reduction step **(b)**.

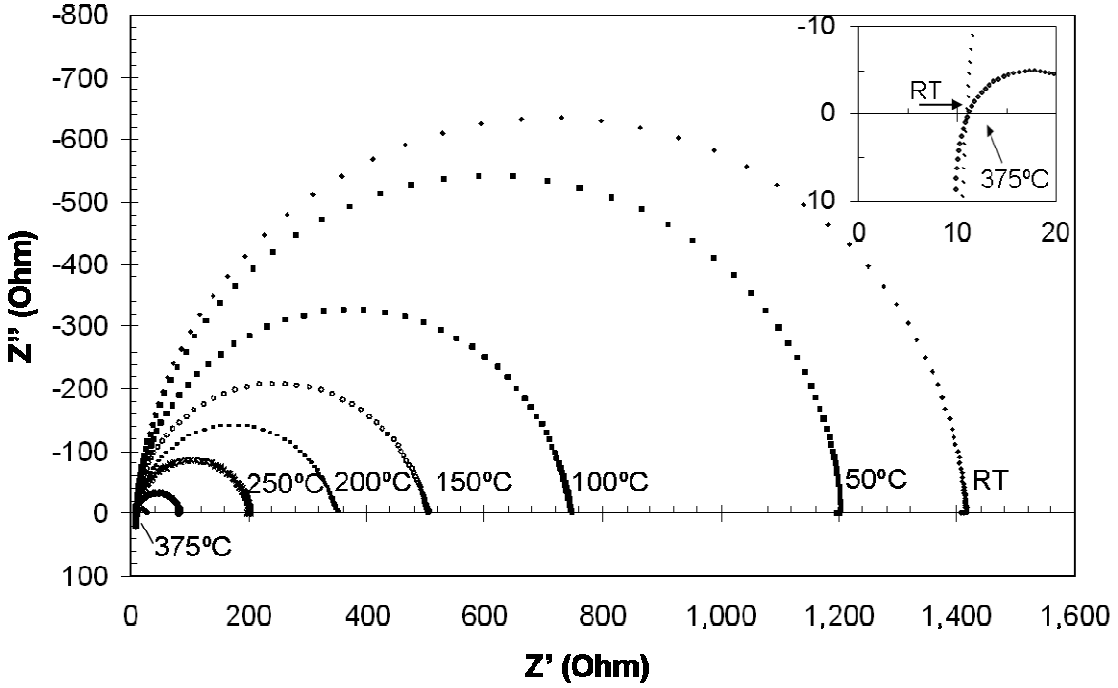

Figure 3. Impedance plot for Ti_nO_{2n-1} (1MHz to 0.1Hz, RT to 375ºC). The inset shows the non-zero intercept on the Z' axes, from which the resistance (R_B) of the grain bulk can be obtained. The only observable arch is attributed to the grain boundaries (R_{GB}) response.

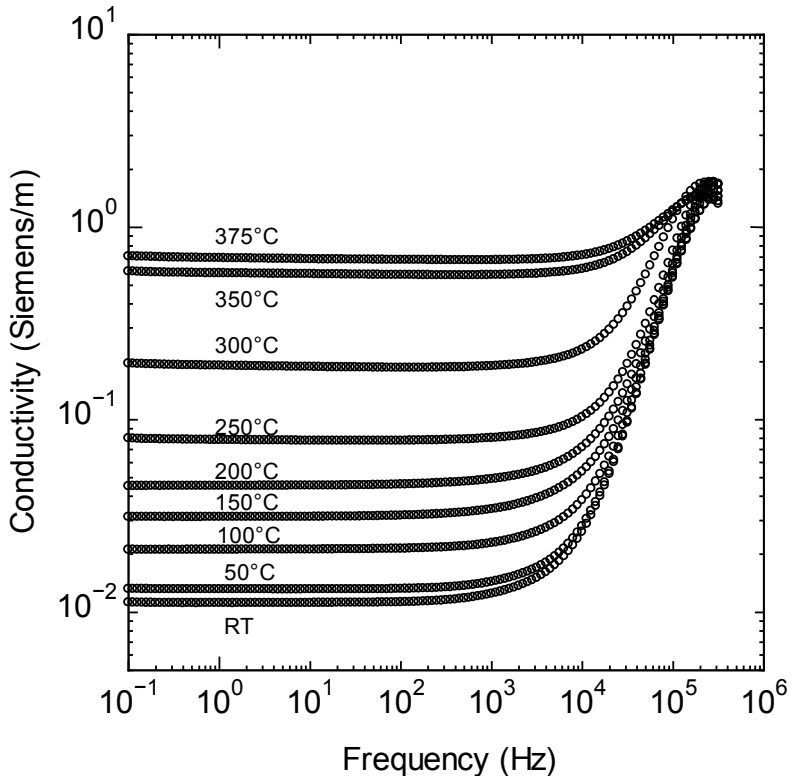

Figure 4. Ac conductivity of Ti_nO_{2n-1} (0.1Hz to 1MHz, RT to 375°C). The conductivity increases with temperature and it is frequency dependent at frequency higher than 1-10kHz.

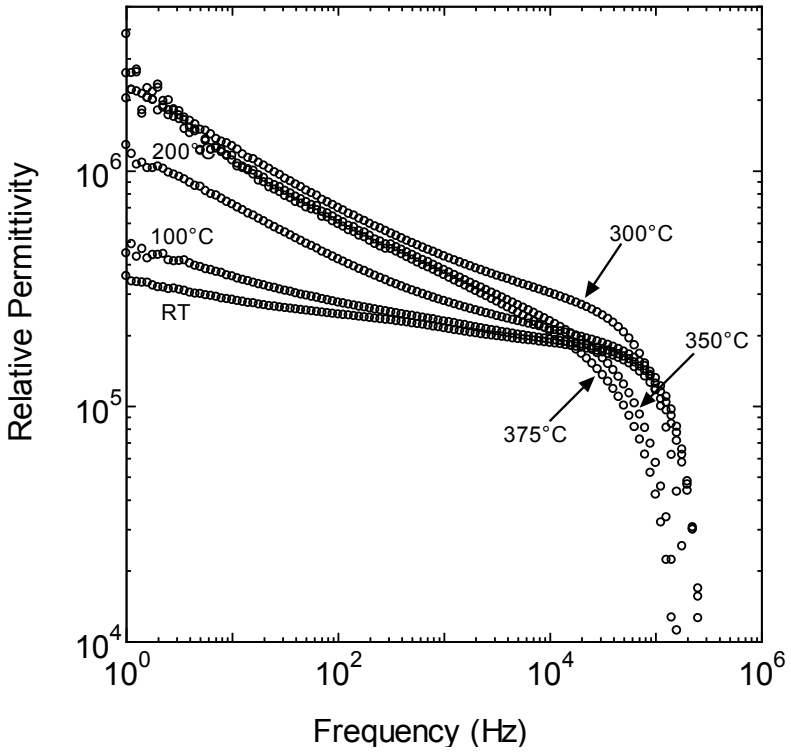

Figure 5. Relative Permittivity of Ti_nO_{2n-1} (1Hz to 100KHz, RT to 375°C). At lower temperature (<300°C) the permittivity is frequency independent, before dropping abruptly at 10-100KHz. At higher temperature (>300°C) the resistivity of the grain boundaries drops and a power law dependence from frequency is observed.